Measurement of low-energy total absolute atomic collision cross sections with the metastable $^3P_2$ state of neon using a magneto-optical trap

K. J. Matherson, R. D. Glover, D. E. Laban, and R. T. Sang*
Centre for Quantum Dynamics, Griffith University, Nathan, Queensland 4111, Australia
(Received 6 February 2008; published 28 October 2008)

We present total absolute collision cross sections for neon in the $^3P_2$ metastable state with ground state, thermal atoms and molecules using a recently developed experimental technique. The technique utilizes a magneto-optical trap (MOT) and involves the measurement of MOT population dynamics to determine the cross section. Collision cross section measurements are presented for metastable neon in the $^3P_2$ state with He, Ne, Ar, H_2, O_2, and N_2. The average thermal energy of the collision ranges from 11 to 27 meV. The measurements made using this technique have small errors, of the order of 10% of the measured cross section; the technique is capable of producing benchmark collision cross sections.

DOI: 10.1103/PhysRevA.78.042712 PACS number(s): 34.50.−s

The study of atomic collision processes provides important information for a number of research applications, such as plasma physics and astrophysics. These interactions are also important to practical applications and new technologies, such as lasers, plasma televisions, and electrical discharges [1]. The data produced by experimentally measuring these processes in the form of collision cross sections provide a means of rigorously testing theoretical quantum mechanical calculations. Metastable noble gases are especially interesting since the energy content of these excited states is higher than the ionization potential of most known atomic and molecular species, and their lifetimes are much longer than typical collision times in the gas phase [2]. These collisions are also of general interest in excited state chemistry [3]. Metastable states also play a role in the transfer of excitation via collisions and can mediate changes in the internal states of other atoms, a process used in devices such as the HeNe laser.

In this investigation the average thermal energy of the collisions is between 11 and 27 meV. At these energies the dominant interaction between a metastable and ground state atom during a collision event is the elastic scattering process (1). Other possible collision processes are associative ionization (2) and Penning ionization (3):

$$\mathrm{Ne}^* + X \rightarrow \mathrm{Ne}^* + X, \tag{1}$$

$$\mathrm{Ne}^* + X \rightarrow \mathrm{Ne}X^+ + e, \tag{2}$$

$$\mathrm{Ne}^* + X \rightarrow \mathrm{Ne} + X^+ + e. \tag{3}$$

Experimental investigations of such collision processes are traditionally carried out using a crossed-beam technique. In these experiments two perpendicular collimated atomic (or molecular) beams are crossed in a well-defined interaction region and the products of collisions are then detected. Detailed studies have been carried out for metastable rare gas systems with various other noble gas atoms, diatomics, molecules, and electrons using a crossed-beam technique [4–11]. Total ionization cross section measurements as well as Penning and associative ionization cross section measurements have been performed for mixed and unmixed metastable Ne in the $^3P_2$ and $^3P_0$ states [2,3,12,13]. Differential elastic cross sections have been measured for some metastable systems using the crossed-beam method [14–16]. The angular resolution is provided by a narrow slit placed before the scattered particle detector [17]. The technique is quite useful for differential cross section measurements but absolute cross sections are difficult to determine since the absolute number of target atoms as well as the the overlap volume of the beams is required to be known accurately. This is a major source of error for this type of experiment [18]. Velocity-dependent elastic cross sections have been made for noble gases with other atoms and molecules using velocity-selected beams to alter the interaction energy [15,19]. Rothe *et al.* [20,21] have measured total absolute collision cross sections of metastable He and Ne at large average relative velocities of 1000–3000 ms^{-1} using a beam-gas attenuation method.

In this paper, we present measurements for the total absolute collision cross section between cold Ne* in the $^3P_2$ metastable state and room temperature (295 K) He, Ne, Ar, H_2, O_2, and N_2. The experiment was carried out using a magneto-optical trap (MOT) where Ne in the $^3P_2$ metastable state is confined in a potential well of approximately 4 mK. The total absolute collision cross section is measured using a technique that has been recently developed [22]. The method is based upon the principle that the collision cross section between the trapped atoms and a collision species can be determined by measuring the trap loss rate. This is achieved by introducing a collision species into the trapping region thus increasing the number of collision events. Collisions where associative or Penning ionization take place removes an atom from the trap as the Ne is left with an internal quantum state that is insensitive to the MOT trapping force. Elastic collisions lead to trap loss if sufficient collisional momentum is transferred from the hot collision species to the trapped metastable Ne atoms. At relatively low energies the total ionization cross section for Ne* is small compared to the total cross section (see Table I) therefore elastic collisions are the dominant trap loss mechanism. To make a measurement, the trap loading is turned off and the change in the loss

*R.Sang@griffith.edu.au

TABLE I. The total absolute collision cross section from metastable Ne in the $^3P_2$ state.

Species	$\bar{\nu}$ (m.s^{-1})	Relative Collision Energy (meV)	σ_M (Å^2)[a]	σ_R (Å^2)[b]	σ_{TI} (Å^2)[c]
He	1249.0	27.0	$164.8 \pm 0.5 \pm 15.5$	123	
Ne	556.3	16.2	$499.1 \pm 4.1 \pm 47.1$	143	
Ar	395.4	10.9	$837.7 \pm 15.7 \pm 79.0$	398	3.46–30.5
H_2	1760.0	29.4	$230.1 \pm 2.8 \pm 21.7$		2.6–23.4
O_2	441.8	12.5	$1026.8 \pm 12.7 \pm 96.9$		25.5
N_2	472.1	13.5	$1259.0 \pm 16.5 \pm 118.8$		10.4

[a]Measurements are for this work. The errors quoted are, respectively, the statistical and systematic errors.
[b]Measurements are from [21], the average collision energy for these measurements is significantly higher (~115 meV), and the quoted error is estimated to be on the order of 25%.
[c]The total ionization cross section for collision with metastable Ne in a mixed composition of $^3P_2$ and $^3P_0$ [6] have been included for comparison purposes. The relative collision energies are between 33 and 47 meV.

rate is measured by observing the population dynamics of the trapped atoms as the MOT decays. The advantage of performing these studies using this method is that the MOT provides a pure source of Ne in the $^3P_2$ metastable state. It is also advantageous that no knowledge of the trap population or overlap volume is required; it is only necessary for the loss rate and absolute density of the collision species to be measured. This technique is similar to a method used to measure photoionization cross sections [23,24], total absolute electron-atom collision cross sections [25], and total absolute ionization cross sections from Rb [26].

The rate of change of the number of trapped atoms is determined by the loading and the loss rates of the trap. In a low-density MOT, where the spatial distribution in the trap is Gaussian, it is given by [27]

$$\frac{dN_t}{dt} = R_L - N_t(\Gamma_B) - \frac{\beta N_t^2}{V_{\text{eff}}}, \tag{4}$$

where N_t is the number of trapped metastable Ne atoms, R_L is the loading rate of the trap, Γ_B is the trap loss rate due to collisions with residual background gas atoms, β is the density-dependent loss rate for collisions between trapped atoms, and $V_{\text{eff}}=8\pi^{3/2}w$ with w being the full width at half maximum of the trap distribution. The addition of a collision species to the trapping region changes the population dynamics and hence Eq. (4) is modified to

$$\frac{dN_t}{dt} = R_L - N_t(\Gamma_B + \Gamma_C) - \frac{\beta N_t^2}{V_{\text{eff}}}, \tag{5}$$

where Γ_C is the additional loss rate due to the introduced collision species. The cross section σ, for collisions between the trapped atoms and the collision species, can be found by measuring Γ_C and is given by [28]

$$\sigma = \frac{\Gamma_C}{n\bar{\nu}}, \tag{6}$$

where n is the density of the collision species and $\bar{\nu}$ is the relative collision velocity, which can be approximated as the mean velocity of the collision species and is given by

$$\bar{\nu} = \sqrt{\frac{8k_BT}{\pi m}}, \tag{7}$$

where T is the temperature and m is the mass of the collision species. If the loading rate R_L is set to zero then the decay from steady state can be found by solving Eq. (5), which yields

$$N_t(t) = \frac{N_t(0)e^{-t(\Gamma_B+\Gamma_C)}}{1+[\beta N_t(0)/V_{\text{eff}}(\Gamma_B+\Gamma_C)](1-e^{-t(\Gamma_B+\Gamma_C)})}. \tag{8}$$

The loss rate due to collisions with the introduced collision species Γ_C, can be found by fitting Eq. (8) to the measured trap decay. The cross section can then be found by plotting Γ_C as a function of n, the absolute density of the collision species. This is a linear relationship [Eq. (6)] where the gradient is proportional to the collision cross section σ.

The apparatus used for the experiment has been described in detail elsewhere [22] and can be seen in Fig. 1. Briefly, a beam of metastable Ne atoms is created in a hollow cathode discharge-type source that is liquid nitrogen cooled to reduce the mean atomic thermal velocity to 500 ms^{-1}. The metastable atom flux from the source is approximately 1×10^{14} atoms sr^{-1} s^{-1}. The beam of atoms is subsequently longitudinally slowed to approximately 20 ms^{-1} using a counterpropagating red-detuned laser beam combined with a Zeeman slower. The atoms are then trapped in the MOT, which consists of three retroreflected, orthogonal, circularly polarized, 25-mm-diameter laser beams, red detuned from the cooling transition by typically three linewidths. The trapping field has a typical magnetic gradient of 0.25 T m^{-1}. The cooling transition is 640.4 nm from the $^3P_2$ metastable state to the $^3D_3$ excited state with a saturation intensity I_0 of 4.2 mW cm^{-2} [27]. The lifetime of the $^3P_2$ metastable state is 14.7 s [29], which is much longer than any measurement being made and so can be treated as an effective ground state. The excited $^3D_3$ state has a lifetime of 18.7 ns [27]. Decay from the $^3D_3$ state is possible only via a single channel to the $^3P_2$ state and is a "closed transition," that is, only these two states play a role in the optical process.

The observed spherical atom cloud typically consists of approximately 10^7 atoms with a diameter of 2 mm. The fluorescence from the trapped atoms is used to monitor the popu-

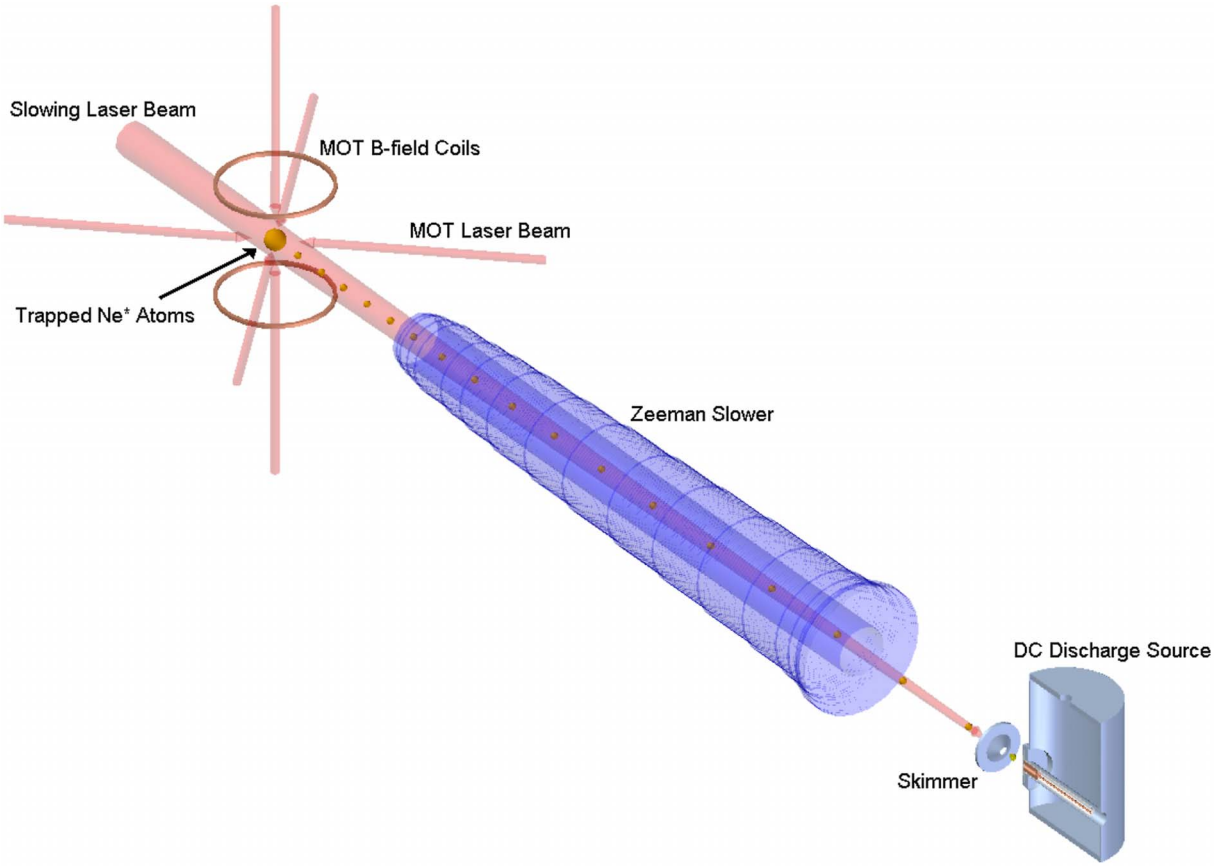

FIG. 1. (Color online) Schematic of the Ne* trap apparatus, including, the metastable Ne source, Zeeman slower, trap *B*-field coils, and associated laser beams.

lation dynamics. A 12-bit charge-coupled device camera with an external optics system to provide 10× magnification is used to measure the fluorescence.

The collision species is introduced into the trap chamber via stainless steel gas lines with the flow controlled by a variable leak valve. The background pressure of the MOT vacuum chamber during operation is typically 10^{-8} Torr. The partial pressure of the introduced species is monitored using a calibrated residual gas analyzer (RGA). The technique requires the absolute pressure of the collision species to be known accurately. The calibration of the RGA in the pressure range of interest (10^{-7}–10^{-9} Torr) was performed by the dynamic expansion method [30] for each gas species. The dynamic expansion method is utilized in vacuum systems that are permanently evacuated by vacuum pumps. Full calibration details are given in previous work [22]. The pressure calibration is the largest contribution to error for this technique and results in an error of 8% of the measured density of the collision species.

Two other processes contribute to the measurement error, the excited state fraction of the trapped atoms and recapture after a small angle scattering event. Error due to the excited state fraction is a result of the trapping laser beams remaining in operation during the measurement. The measured cross section will therefore have a contribution from both the $^3P_2(m_J=2)$ metastable state and the $^3D_3(m_J=3)$ excited state. Typical operating parameters ($I \approx 2I_0$, $\delta \approx 3\gamma$) yield a calculated excited state fraction of 1.4% of the total trapped atoms. This leads to an error in the measured $^3P_2$ cross section of only a few percent [22].

The small angle scattering error is due to recapture of an atom after a scattering event. Recapture can occur if the momentum transferred to a trapped atom, in an elastic collision event, results in a velocity gain that is less than the escape velocity of the trap. In this case the atom has undergone a collision; however, the collision will not contribute to the measured cross section.

The contribution to the error due to both of these processes can be estimated by changing the trapping parameters. In order to achieve this, the trapping laser beams are further red detuned altering the excited state fraction and the escape velocity of the trap. The escape velocity of the trap ranges from approximately 5 to 35 ms^{-1} depending on the detuning. For the case when the escape velocity is 5 ms^{-1}, the minimum scattering angle for Ar can be calculated to be approximately 30 mrad. The critical angle for small scattering angle resolution is given by [31]

$$\theta_c = \frac{\pi\hbar}{\mu v_{\mathrm{rel}}(\sigma_{\mathrm{tot}}/2\pi)^{1/2}}. \tag{9}$$

For Ar at 400 ms^{-1}, $\theta_c \approx 30$ mrad, which implies that the majority of the small angle scattering events are resolved. The relative error associated with missing small angle elastic

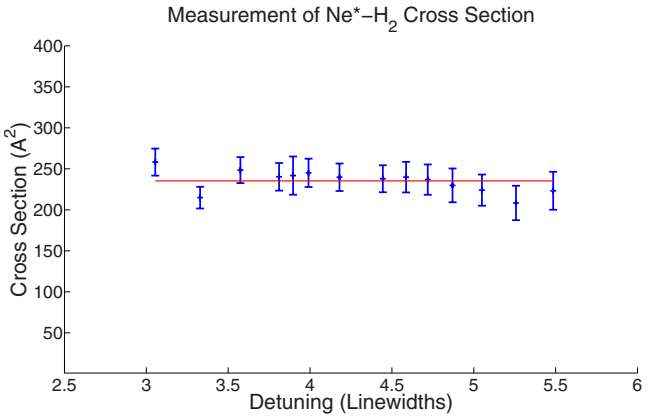

FIG. 2. (Color online) Total absolute collision cross section of Ne* in the $^3P_2$ state and H_2 as a function of the trapping laser detuning. The straight line indicates the averaged cross section value. The data show no significant dependence on detuning.

scattering is then 1% [32]. The same analysis can be carried out for He and yields a smaller error of 0.1%.

Figure 2 is a typical graph of the cross section as the detuning of the trapping laser is varied. This data shows no change of statistical significance, suggesting that the contribution to the cross section from both the excited $^3D_3$ state and the small angle scattering is not significant compared to the total error.

Results are taken by measuring the total decay rate (due to collisions with background atoms and the collision species) $(\Gamma_B+\Gamma_C)$ as a function of the absolute density of the collision species, n. The collision cross section can then be found from Eq. (6), as described previously. The decay rates are measured multiple times (>10) at each pressure to reduce the statistical error of the measurement. A fit to the data gives the cross section with a fitting error of approximately 2–10 %. Repeating this measurement multiple times and taking a weighted average of the data reduces the statistical error to ~1%. As stated previously, the most significant contribution to the error is due to the measurement of the absolute density of the collision species (8%). This error is added in quadrature to a systematic error of 5%, which is included to account for errors due to the excited state fraction and small angle scattering. Table I gives the measured cross sections between metastable Ne in the $^3P_2$ state and the ground states of He, Ne, Ar, H_2, O_2, and N_2. Previously reported data for metastable Ne collisions with Ar [22] have been updated due to an error in the density measurement for this rare gas. It should be noted that the cross section for Ne*-He is completely elastic since the metastable Ne atom does not contain enough energy to ionize the He atom.

At low velocities it is expected that elastic, van der Waals type interactions should dominate and the cross section can be approximated as [31]

$$\sigma_{\mathrm{tot}}(v_{\mathrm{rel}}) \approx 8\left(\frac{C_6}{\hbar v_{\mathrm{rel}}}\right)^{2/5}. \tag{10}$$

To estimate the total cross section over the velocity range, the rate of collisions leading to trap loss is calculated for each velocity using Eq. (10) and integrated from the capture velocity of the MOT over the Maxwellian distribution. The result can then be compared with the experimentally measured cross section. This approximation should be most accurate for the Ne*-He interaction since the cross section is entirely elastic. Using this method and C_6 equal to 340 kcal mol^{-1} Å^6 [33], the total elastic cross section for metastable Ne in the $^3P_2$ state with thermal ground state He can be calculated to be 168.9 Å^2. This value lies within the error for the experimentally measured cross section value and further validates the cross sections measured in this work.

We believe this measurement to be unique due to the low energy of the collision and the relatively low error of each measurement. For comparison purposes, the only similar measurement from the literature is that of Rothe *et al.* [21] (Table I). In that work the total absolute collision cross sections for metastable Ne in the $^3P_2$ state with thermal rare gases are measured at approximately four times the collision energy used in our work. The cross sections are roughly the same order of magnitude as our work but are consistently smaller. This is not a surprising result given the higher energies of the collision partners, since a trend exists for the elastic cross section to decrease with an increase in collision energy [34]. It should be noted that the sources of error in the Rothe *et al.* [21] measurements are roughly estimated to be 25% of the measured cross section. We believe that our technique yields vastly superior measurement errors of approximately 9.5% of the measured cross section.

This research was supported by the Australian Research Council and Griffith University. K.J.M., R.D.G., and D.E.L. were supported by the Australian Research Council.

[1] G. Veronis, U. S. Inan, and V. P. Pasko, IEEE Trans. Plasma Sci. **28**, 1271 (2000).
[2] A. Aguilar, S. Bianco, B. Brunetti, M. Gonzalez, and F. Vecchiocattivi, Mol. Phys. **71**, 897 (1990).
[3] A. Aguilar-Navarro, B. Brunetti, S. Rosi, F. Vecchiocattivi, and G. G. Volpi, J. Chem. Phys. **82**, 773 (1985).
[4] R. H. Neynaber and G. D. Magnuson, Phys. Rev. A **11**, 865 (1975).
[5] A. Niehaus, Adv. Chem. Phys. **45**, 399 (1981).
[6] A. J. Yencha, *Electron Spectroscopy: Theory Technique, and Application*, edited by C. R. Brundle and A. D. Baker (Academic Press, New York, 1984), Vol. 5.
[7] H. Hotop, *Electronic and Atomic Collisions* (North-Holland, Amsterdam, 1980), p. 271.
[8] P. E. Siska, Rev. Mod. Phys. **65**, 337 (1993).
[9] M. Jacka, J. Kelly, B. Lohmann, and S. J. Buckman, J. Phys. B

28, L361 (1995).
[10] A. Siegel, J. Ganz, W. Buβert, and H. Hotop, J. Phys. B **16**, 2945 (1983).
[11] R. Kau, I. D. Petrov, V. L. Sukhorukov, and H. Hotop, J. Phys. B **29**, 5673 (1996).
[12] W. P. West, T. B. Cook, F. B. Dunning, R. D. Rundel, and R. F. Stebbings, J. Chem. Phys. **63**, 1237 (1975).
[13] B. Brunetti, S. Falcinelli, A. Sassara, J. de Andres, and F. Vecchiocattivi, Chem. Phys. **209**, 205 (1996).
[14] R. W. Gregor and P. E. Siska, J. Chem. Phys. **74**, 1078 (1981).
[15] J. Baudon, P. Feron, C. Miniatura, F. Perales, J. Reinhardt, and J. Roberts, J. Chem. Phys. **95**, 1801 (1991).
[16] H. Haberland, Y. T. Lee, and P. E. Siska, Adv. Chem. Phys. **45**, 487 (1981).
[17] P. Feron, F. Perales, B. Decomps, J. Robert, J. Reinhardt, and J. Baudon, Chem. Phys. Lett. **160**, 555 (1989).
[18] F. J. d. Heer and M. Inokuti, *Electron Impact Ionization* (Springer-Verlag, New York, 1985).
[19] E. R. T. Kerstel, M. F. M. Janssens, K. A. H. V. Leeuwen, and H. C. W. Beijerinck, Chem. Phys. **119**, 325 (1988).
[20] E. W. Rothe, R. H. Neynaber, and S. M. Trujillo, J. Chem. Phys. **42**, 3310 (1965).
[21] E. W. Rothe and R. H. Neynaber, J. Chem. Phys. **42**, 3306 (1965).
[22] K. J. Matherson, R. D. Glover, D. E. Laban, and R. T. Sang, Rev. Sci. Instrum. **78**, 073102 (2007).
[23] T. P. Dinneen, C. D. Wallace, K. Y. N. Tan, and P. L. Gould, Opt. Lett. **17**, 1706 (1992).
[24] B. J. Claessens, J. P. Ashmore, R. T. Sang, W. R. MacGillivray, H. C. W. Beijerinck, and E. J. D. Vredenbregt, Phys. Rev. A **73**, 012706 (2006).
[25] R. S. Schappe, P. Feng, L. W. Anderson, C. C. Lin, and T. Walker, Europhys. Lett. **29**, 439 (1995).
[26] R. S. Schappe, T. Walker, L. W. Anderson, and C. C. Lin, Phys. Rev. Lett. **76**, 4328 (1996).
[27] H. J. Metcalf and P. V. d. Straten, *Laser Cooling and Trapping* (Springer-Verlag, New York, 1999).
[28] E. W. McDaniel, *Atomic Collisions* (Wiley, New York, 1989).
[29] M. Zinner, P. Spoden, T. Kraemer, G. Birkl, and W. Ertmer, Phys. Rev. A **67**, 010501(R) (2003).
[30] W. Umrath, *Fundamentals of Vacuum Technology* (Leybold, Cologne, 1998).
[31] J. J. H. van den Biesen, *Atomic and Molecular Beam Methods* (Oxford University Press, Oxford, 1988), Vol. 1, p. 472.
[32] H. Pauly, Z. Phys. **157**, 54 (1959).
[33] T. Fukuyama and P. Siska, Chem. Phys. Lett. **39**, 418 (1976).
[34] J. E. Cohen and B. Schneider, Phys. Rev. A **11**, 884 (1975).